ISSN: 2664-9640

Vortex-induced vibration characteristics of a wind energy harvesting device

Yuanli Chen, Yuwang Song, Wei Liu, Hu Wang

School of Energy Power and Mechanical Engineering, North China Electric Power University, Beijing, 102206, China

Abstract

An electromagnetic power generation device based on air fluid vortex-induced vibration (VIV) was designed and its vortex-induced vibration (VIV) characteristics were studied. A series of cylindrical blunt bodies with diameters of 40 mm, 50 mm, 60 mm and 70mm were designed. The resonant frequencies and locked wind speeds were obtained by theoretical formula and fluid-structure interaction analysis, and the analysis results were verified by physical experiments. Among them, the resonance frequency of 60mm cylindrical blunt body is 3.13Hz at 1m/s locking wind speed, the amplitude is ±5.6cm, and the energy conversion efficiency reaches 77.38%, which lays a technical foundation for the subsequent system research on the power generation characteristics of the whole machine.

Keywords

Vortex-induced vibration; Wind energy harvesting; Electromagnetic; Vibration response; Wind tunnel experiments.

1. Introduction

Mechanical vibration is a common form of energy in the environment. Vibration energy collector is an all-weather power supply device for various low-power electronic devices by converting the vibration energy widely existing in nature. Due to the characteristics of small size, long life and high energy density, all kinds of vibration energy collectors are developing rapidly and becoming one of the important micro-energy devices that are widely studied at present [1]. At present, this kind of technology can be divided into electromagnetic, piezoelectric, electrostatic, magnetostrictive and composite types [2]. It is mostly used in micro-electro-mechanical systems (MEMS) to supply power to sensor nodes or other wechat electronic components by collecting micro-vibration energy in nature instead of traditional chemical batteries or power lines [3-5].

In addition to MEMS, vibratory energy power generation is also used in larger scale power generation, such as flow-induced vibration acquisition technology based on wind or water power, with Vortex-induced Vibrations, Galloping, Four fluid-induced vibrations, including flutter and buffeting, act as energy collection mechanisms [6].Yili Hu et al. [7] proposed a piezoelectric flow energy collector (PFEH, Harvester), which uses a cylindrical blunt body to generate vortide-induced vibration in the wind field and drive the vibration of piezoelectric cantilever beam to generate electricity. Jos et al. [8] constructed a model of galloping based piezoelectric wind energy harvester (GPWEH) with peripheral structure to collect energy by using galloping phenomenon generated by a blunt body with non-cylindrical cross-section in the wind field.Sun W et al and Junlei Wang[9-10] et al realized the transformation from VIV to GALLOping vibration by adding accessories on the surface of blunt body or changing the cross-section shape of blunt body respectively.In the above studies, the electromechanical energy conversion structure (power generation structure) adopts the form of piezoelectric cantilever

ISSN: 2664-9640

beam, that is, the piezoelectric layer and protective layer are pasted on the metal base (aluminum or stainless steel, etc.), and the positive piezoelectric effect is used to generate electricity when the blunt body drives the cantilever beam to vibrate. However, the piezoelectric structure has certain defects, such as hard and brittle piezoelectric materials, limited bearing capacity, easy to produce fatigue damage, depolarization phenomenon, low electromechanical coupling coefficient, to a certain extent, reduce the energy conversion efficiency and so on. Therefore, the electromagnetic power generation structure with coil and permanent magnet as the main body is designed, which has the advantages of high sensing frequency of electromagnetic vibration energy collector, simple process, convenient manufacture, easy analysis and can be applied to all kinds of harsh environment.

The wind energy acquisition device studied in this paper adopts a single freedom of freedom vibration acquisition structure with a blunt cylinder connected to a cantilever beam, and combines the electromagnetic power generation structure to collect and transform the energy. Under different wind conditions and different application conditions, based on the viV mechanism, the vibration of bluff body in wind field is simulated and physical experiment is carried out to study the vibration law of bluff body in wind field and the power generation characteristics of corresponding motor structure, which will have practical significance for future research and engineering application.

2. Structural design of electromagnetic vibration energy collector

Fig. 1 shows the structure diagram of the electromagnetic vibration energy collector designed, which mainly consists of two parts: one is the viV structure composed of a cylindrical bluff body and a cantilever beam, which is used to convert wind energy into kinetic energy and elastic potential energy of the bluff body and the flexible rod; The other is the electromechanical coupling structure composed of coils, permanent magnets and their respective installation devices, which is used to convert mechanical energy into electrical energy to achieve the purpose of generating electricity.

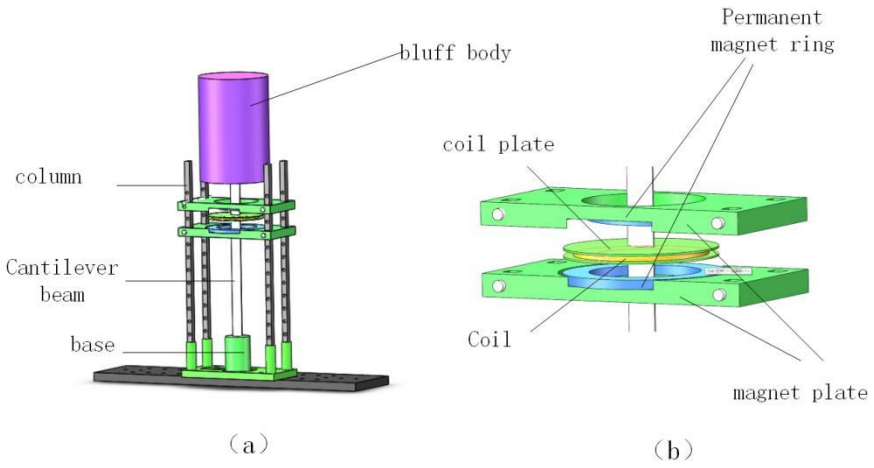

Fig.1 (a) Schematic diagram of the structure of an electromagnetic vibration energy harvester (b) Schematic diagram of electromechanical coupling structure

According to the different vibration units fixed on the cantilever beam, it is divided into two types: moving iron type and moving coil type. In order to make full use of the magnetic field of the permanent magnet, a moving coil structure is adopted in the design, that is, the cantilever beam drives the coil to vibrate, so that it cuts the magnetic field lines between the two magnetic rings, thereby generating a moving electromotive force. The pole is used to fix the magnetic ring and adjust the height of the magnet plate, so that the device can complete energy collection in

ISSN: 2664-9640

different vibration positions. Multiple sets of magnetic rings can be installed at different working heights through the column with holes (a pair of magnetic rings is shown in the figure) to improve the power generation efficiency of the system. The coil is fixed on the cantilever beam through the coil panel. When winding the coil winding, it is initially designed to be arranged in a ring in the horizontal direction, and the thickness of the coil in the vertical direction is minimized, thereby reducing the distance between the two magnetic rings and increasing the Magnetic induction between the magnetic rings.

3. Study on Vortex-Induced Vibration Structure

3.1. Theoretical Analysis of Vortex Induced Vibration

For the vibration structure of the designed device, its governing equation can be expressed as:

$$M_{eq}\ddot{Z}(t)+C_{eq}\dot{Z}(t)+K_{eq}Z(t)=F_L \tag{1}$$

In formula (2), F_L is the lift force of the fluid acting on the structure. According to the research of Li Baoqing [11], the lift force FL is expressed as:

$$F_L=\frac{1}{2}\rho U^2 DLC'_L \sin(\omega_s t) \tag{2}$$

In formula (3), L is the length of the cylinder under force; C'_L is the mean square root of the lift coefficient; D is the diameter of the cylinder; ρ is the density of the fluid; U is the fluid velocity; fs is the vortex shedding frequency on the surface of the cylinder, and it can be expressed as

$$f_s=\frac{S_t\times U}{D} \tag{3}$$

In the formula, St is the Strohha number, which is a relatively stable dimensionless parameter, and also has a certain relationship with the Reynolds number. In the range of 200-2×105 Reynolds number, the Strohha number St is basically kept around 0.2.

In addition, in formula (1), Z(t) is the vibration response displacement of the equivalent mass of the cantilever beam and the bluff body; M_{eq}, C_{eq}, and K_{eq} are the equivalent mass, equivalent damping, and equivalent stiffness of the vibration pickup structure, respectively.

$$C_{eq}=2\xi M_{eq}\omega_n \tag{4}$$

In formula (5), ω_n is the natural angular frequency of the vibrating structure, $\omega_n=2\pi f_n$, f_n is the natural frequency of the vibrating structure, and ξ is the relative damping coefficient.

Substituting formula (2) and formula (4) into formula (1), we can get:

$$M_{eq}\ddot{Z}(t)+2M_{eq}\omega_n\xi\dot{Z}(t)+K_{eq}Z(t)=\frac{1}{2}\rho U^2 DLC'_L\sin(\omega_s t) \tag{5}$$

When solving a linear ordinary differential equation, it can be assumed that its vibration response is:

$$Z=A_Z\sin(\omega_s t+\varphi) \tag{6}$$

In formula (6), A_Z is the response amplitude; δ is the phase angle, and its expression is $\tan\varphi=2\xi\omega_s\omega_n/(\omega_s^2-\omega_n^2)$, and the formula (6) is brought into the formula (5) to solve, and finally the vibration equation of the vibration structure can be obtained [12]:

ISSN: 2664-9640

$$Z = \frac{\frac{1}{2}\rho D U^2 L C_L' \sin(\omega_s t + \phi)}{K_{eq}\sqrt{[1-(\frac{\omega_s}{\omega_n})^2]^2 + (2\xi\frac{\omega_s}{\omega_n})^2}} \tag{7}$$

It can be seen from equation (7) that the vibration law of the cylindrical bluff body in the wind field is in the form of a sine function, and when the vortex shedding frequency is equal to the natural frequency of the circular tube, the vibration amplitude of the bluff body is the largest, that is, the resonance phenomenon occurs.

From the perspective of power, it can be seen that the power of the fluid flowing through the bluff body is:

$$P_\omega = \rho U^3 DH / 2 \tag{8}$$

where ρ is the fluid density, U is the fluid velocity, and D is the characteristic length of the bluff body, which is its diameter for a cylindrical bluff body.

From equation (6), the vibration displacement of the cylinder can be obtained as

$$Z = A_Z \sin(\omega_s t + \varphi) = A_Z \sin(2\pi f_s + \varphi) \tag{9}$$

where fs is the vortex shedding frequency on the cylinder surface.

The power absorbed by the bluff body can be expressed as :

$$P_c = \frac{1}{T}\int_0^T F_L \dot{Z} dt、= \frac{1}{T}\int_0^T (M_{eq}\ddot{Z}(t) + C_{eq}\dot{Z}(t) + K_{eq}Z(t))\dot{Z} dt = 8\pi^3 M_{eq}\zeta(A_Z f_s)^2 f_n \tag{10}$$

where ζ is the relative damping coefficient, and fn is the natural frequency of the vibrating structure. Then the conversion efficiency of the vibration structure can be obtained as [13]:

$$\eta_b = \frac{P_c}{P_\omega} = \frac{16\pi^3 M_{eq}\zeta(A_Z f_s)^2 f_n}{\rho U^3 DH} \tag{11}$$

3.2. Numerical simulation and result analysis

It is known from the principle of vortex-induced vibration that when the eddy current shedding frequency is close to the natural frequency of the cylinder, it will start to lock to the natural frequency of the cylinder, and will remain locked to this natural frequency even if the flow velocity increases within a certain range. This phenomenon is called locking of vortex shedding, and the vibrating structure has the best vibration effect in the locked state [14]. Therefore, it is necessary to determine the resonance frequency of the bluff body under the locked wind speed, in order to obtain the vibration law of the induction coil under the ideal working state.

First, build 3D models of different sizes, as shown in Figure 2.

The bluff body is defined as EPS plastic foam material, the characteristic lengths are 40mm, 50, 60mm, 70mm, and the height is 180mm. The cantilever beam is defined as aluminum alloy material, and its size is 260mm*15mm*0.8mm, and its different material properties are shown in Table 1.

ISSN: 2664-9640

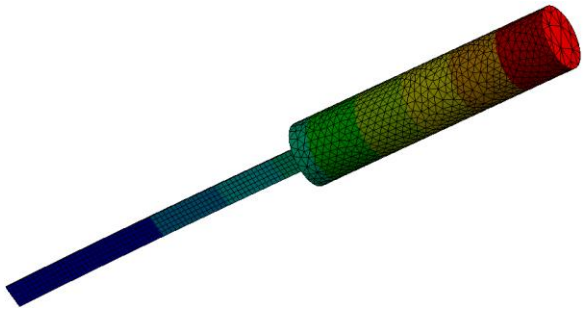

Fig. 2 Modeling and modal analysis of cylindrical bluff body

Tab.1 Material characteristic parameters of vibrating structure

Material	Density/(kg/m^3)	Elastic Modulus/Mpa	Poisson's ratio
Aluminum alloy	2770	71000000	0.33
EPS plastic foam	20	1.52	0.3

The modal analysis and static force analysis are carried out for each model, and the modal parameters such as its natural frequency, equivalent stiffness and equivalent mass are obtained. By formula (3), the natural frequency fn is used to replace the vortex shedding frequency fs, and the Strouhal number 0.2 is used to calculate the locked initial wind speed, that is, the optimal working wind speed of the bluff bodies of different sizes can be obtained, as shown in Table 2.

Tab.2 Vibration structure parameters of different bluff body sizes

Blunt body diameter D/mm	40	50	60	70
Equivalent stiffness K/(N/m)	3.591	3.612	3.621	3.623
Natural frequency fn/Hz	4.772	3.97	3.339	2.888
Locked wind speed U/(m/s)	0.95	0.99	1.00	1.01
Eddy off frequency fs/Hz	4.674	4.005	3.433	3.147
lift coefficient C_L	0.424	0.601	0.672	0.707

In order to verify the correctness of the initial locked wind speed obtained by formula (3), the structural calculation module (Transient structural), the fluid calculation module (Fluent), and the coupling configuration module (System Coupling) in the finite element analysis software ansys were used to try to configure the collector. The vibration process of the fluid-structure interaction analysis is carried out. The cylindrical bluff body vibration pickup structure is placed in the fluid domain, and a single-degree-of-freedom equivalent spring model is added to solve the mutual coupling between the fluid domain and the structure model. The fluid-structure coupling model diagram is shown in Figure 3.

Numerical simulation of bluff body vibration pickup structures with different diameters is carried out. Fig. 4 selects the time-history curve and spectrum analysis of lift coefficient of different bluff bodies under the calculated locked wind speed.

ISSN: 2664-9640

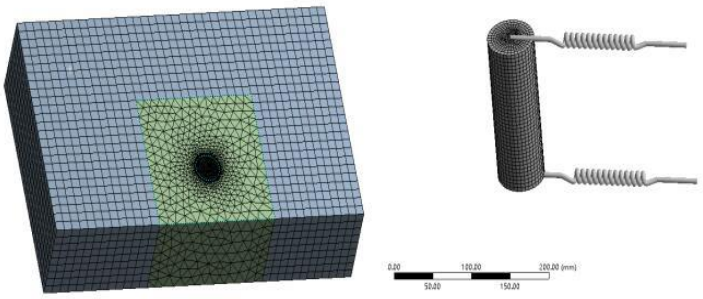

Fig.3 Fluid-structure coupling simulation mesh model

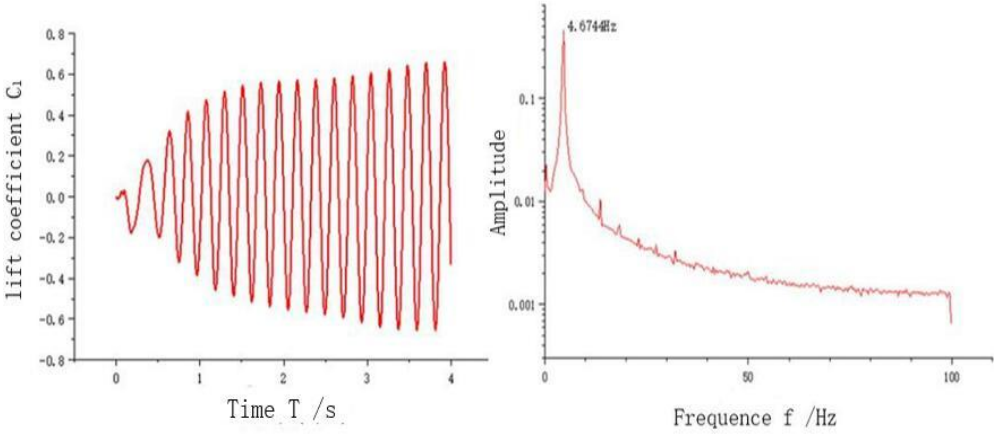

(a)D=40mm

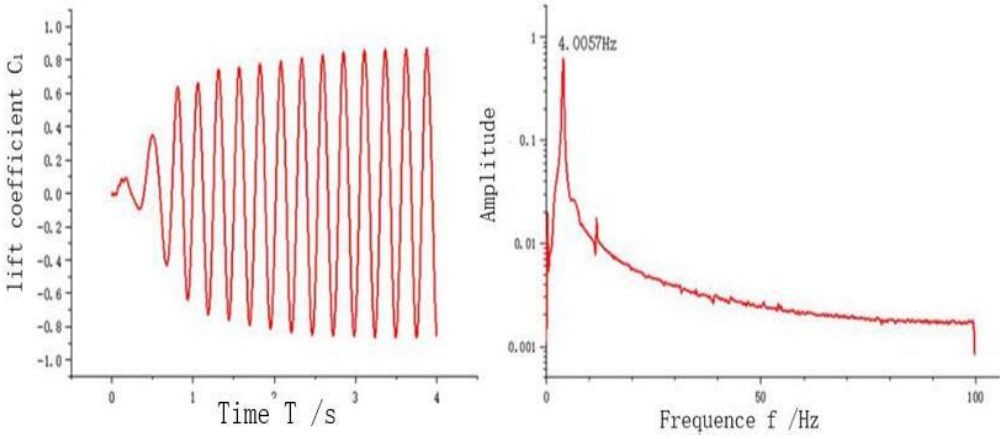

(b)D=50mm

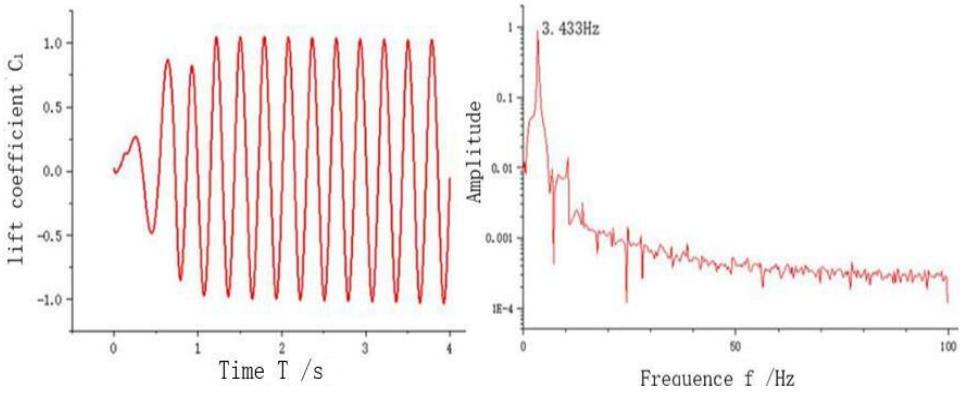

(c)D=60mm

ISSN: 2664-9640

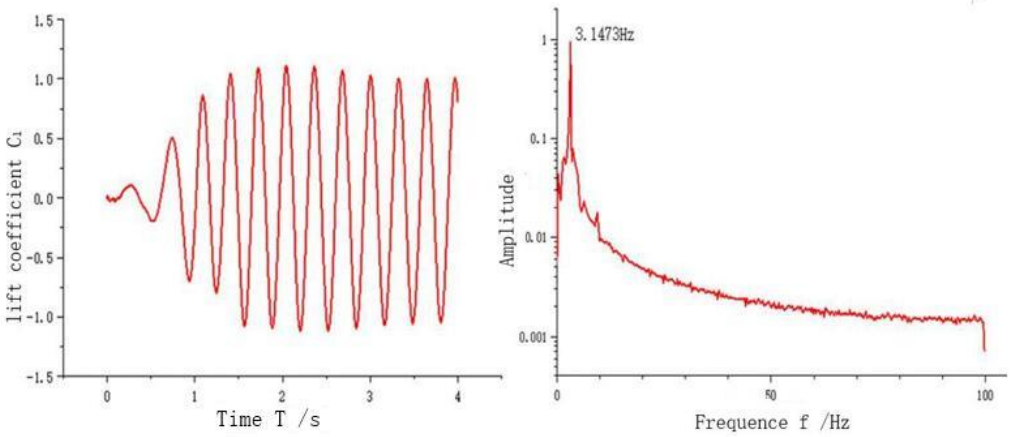

(d)D=70mm

Fig.4 Curve and frequency spectrum analysis of lift coefficient of bluff bodies with different diameters

It can be seen from Fig. 4 that the change of the lift coefficient obtained by the fluid-solid coupling simulation under the locked wind speed is relatively stable, and the change frequency of the lift coefficient, that is, the vortex shedding frequency, is basically consistent with the natural frequency of the modal analysis system, and the errors are 8.2%, 1.5%, 2.6%,8%,respectively. The correctness of the locking wind speed calculated by equation (4) is verified, that is, the bluff body is in a resonance state at this wind speed.

4. Experimental verification and analysis

In order to verify the theoretical analysis and simulation results, an electromagnetic vibration energy harvesting device was designed and fabricated with reference to Figure 1, as shown in Figure 5. The cantilever beam is made of aluminum material, and the cylindrical bluff body is made of high-density EPS foam, which is consistent with the definition of the simulation material.

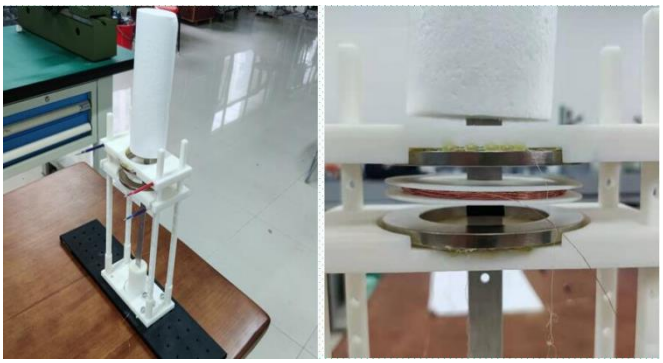

Fig.5 Physical image of vortex-induced vibration energy harvesting device

The overall experimental bench structure is shown in Figure 6. A relatively complete experimental system is built by using laser displacement sensor (Keyence IL-300), simple wind tunnel, anemometer, oscilloscope, and data collector.

ISSN: 2664-9640

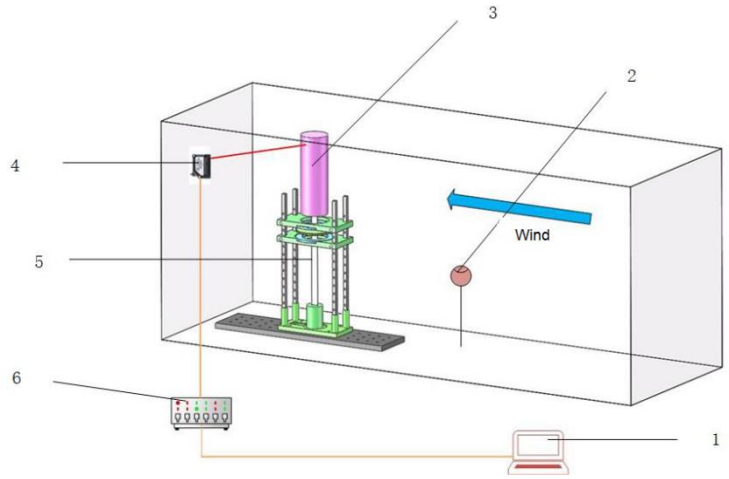

Fig.6 Schematic diagram of the experimental principle of vibration energy harvesting
1 PC terminal 2 Anemometer 3 Wind collecting bluff body 4 Laser displacement sensor
5 Cantilever beam 6 Data collector

The natural frequencies and damping ratios of devices with different diameters were measured by the free vibration attenuation method, as shown in Table 3.

Table 3 Comparison of natural frequency simulation frequency and experimental frequency of different vibration structures

Bluff body diameter D /mm	Simulation frequency/Hz	experimental frequency/Hz	error/%	damping ratio
40	4.772	4.575	4.3	0.0263
50	3.970	3.735	6.3	0.0242
60	3.340	3.230	3.4	0.0183
70	2.888	2.633	8.4	0.0234

It can be seen from the table that there is a certain error between the simulation frequency and the experimental frequency, but they are basically consistent, and the simulation frequency is greater than the experimental frequency. The reason may be the difference between the simulation and the actual experimental environment. For example, the stiffness of the base and the connection stiffness of the cantilever beam and the bluff body are not high enough, which leads to the reduction of the experimental frequency.

Vibration test experiments under different wind speeds were carried out for the vibration pickup devices with different bluff body diameters, and the maximum amplitude of the vortex-induced vibration of the bluff body, the vibration time-history curve and the frequency response data were recorded. It can be seen from Table 2 that the theoretical locking wind speeds of the four sizes of bluff bodies are very close, all around 1m/s, and the experiment found that at the wind speed of around 1m/s, the four types of bluff bodies all produce stable and large amplitude vibrations. The correctness of the calculated resonant wind speed is verified. Taking a bluff body with a diameter of 60 mm as an example, wind speeds of 0.05 m/s, 1 m/s, 3 m/s and 5 m/s are selected to draw the vibration time-history curve and vibration frequency comparison diagram of the system.

It can be seen from Fig.8 that the vibration performance of the cylindrical bluff-body air duct is the best when the wind speed is 1m/s, the amplitude can reach ±5.6cm, and the vibration is

ISSN: 2664-9640

stable, showing obvious sinusoidal motion characteristics. At other wind speeds, the system amplitude is small and unstable, showing a certain "beat" phenomenon. The vibration frequency of the bluff body increases gradually and slowly with the increase of wind speed.

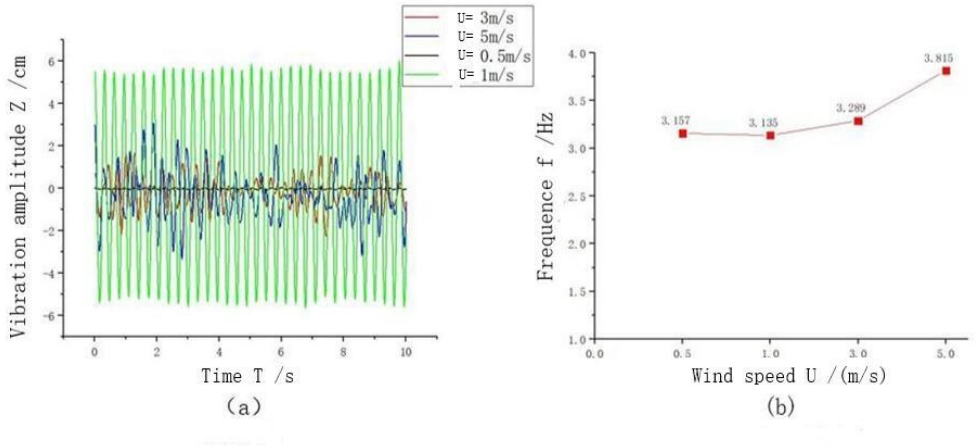

Fig. 7 Vibration structure of a bluff body with a diameter of 60mm under different wind speeds
(a) Comparison of displacement (b) Comparison of vibration frequency

Since the four sizes of bluff bodies all vibrate stably and periodically at a wind speed of about 1 m/s, for the convenience of comparison, the time history of vibration displacement and vibration frequency of 2 seconds are intercepted for comparison, as shown in Figure 8.

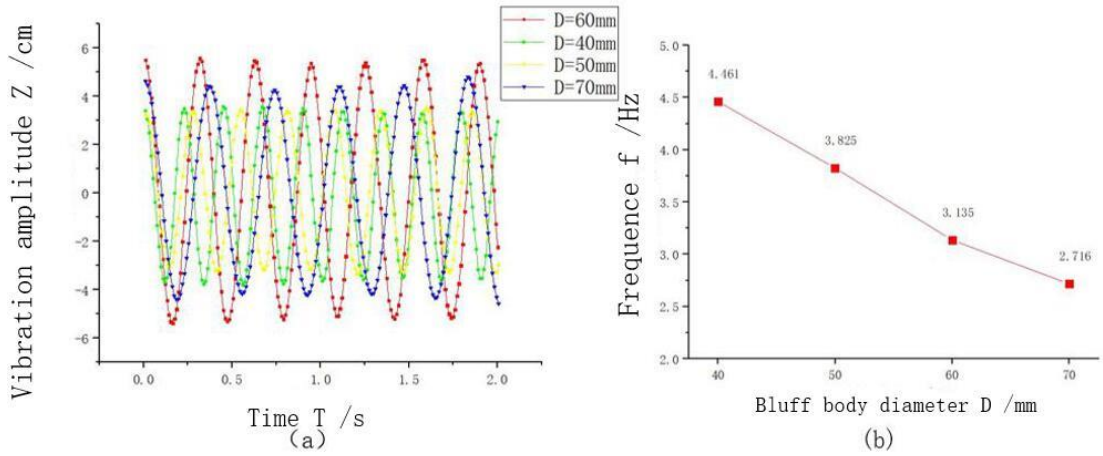

Fig.8 Vibration structure of bluff bodies with different diameters(a) Comparison of displacement (b) Comparison of vibration frequency

By observing Fig.8 (a), it can be seen that the resonance amplitude of the blunt body with the diameter of 60mm is the largest, about ±5.6cm; the resonance amplitude of the blunt body with the diameter of 70mm is slightly smaller, about ±4.5cm; the resonance amplitude of the blunt body with the diameter of 40mm is relatively close, about ±3.5cm.According to Formula (7), Table 2 and Table 4, when the system stiffness, lift coefficient, resonant wind speed and other parameters are close (such as all kinds of blunt bodies with EPS foam materials in the experiment), the resonance amplitude of blunt bodies with different sizes is negatively correlated with their damping ratio. FIG. 8(b) shows that the resonance frequency of the system increases with the increase of the mass of the blunt body, and the resonance frequency is very close to the vortex stripping frequency obtained by fluid-structure coupling simulation and the

ISSN: 2664-9640

natural frequency of the system obtained by attenuation experiment, which verifies the correctness of theoretical calculation of vibration frequency.

According to the resonance amplitude, working frequency, damping ratio and other parameters of the blunt body measured in the experiment, combined with Formula (11), the power conversion efficiency of each vibration structure can be calculated, and the results are shown in Table 4.

Tab. 4 Energy conversion efficiency of different bluff body vibration structures

Bluff body diameterD/mm	40	50	60	70
Fluid flow powerPw/w	0.00441	0.00551	0.00663	0.00772
Cylinder gain power Pc/w	0.0025	0.00267	0.00513	0.0311
Energy conversion efficiency η/%	56.67	48.46	77.38	40.38

As can be seen from the table, the first-order energy conversion efficiency from wind energy to mechanical vibration energy of the four types of energy acquisition devices is high, above 40%, among which the vibration structure with a diameter of 60mm is the highest, reaching 77.38%. It is worth mentioning that a wind speed of 1.5m/s (slightly greater than the locked wind speed) was tested for a 70mm diameter bluff vortex-induced vibration structure, as shown in Fig. 9.

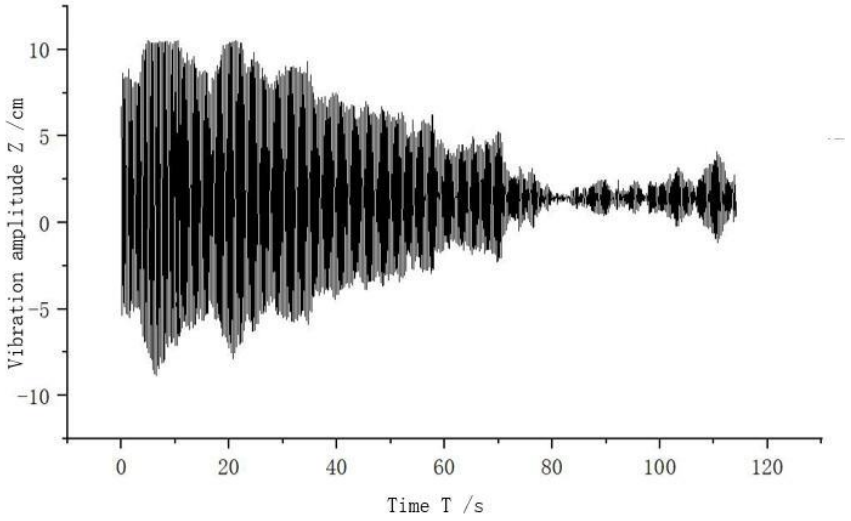

Fig.9 Displacement time history diagram of 70mm diameter bluff body under 1.5m/s wind speed

It is found that in the initial vibration stage, the amplitude of the system was large and relatively stable, reaching ±10cm or so, but with the increase of time, the vibration amplitude gradually decreased, as shown in FIG. 9. After 70s, the vibration became extremely unstable, resulting in "beat" phenomenon. It shows that the system is difficult to maintain a good working condition under the non-locked wind speed. For the vibration energy acquisition system, the system effective bandwidth should be as large as possible. Therefore, for the wind energy acquisition device in this paper, it has become an urgent problem to broaden the wind speed range and effective wind width that the system can work effectively.

ISSN: 2664-9640

5. Summary

(1) The calculated locking wind speed of the bluff body with diameters of 40, 50, 60 and 70mm is close to the experimental value. Taking a bluff body with a diameter of 60mm as an example, its natural frequency theoretical value, actual value and vortex stripping frequency simulation value and actual value are 3.34Hz, 3.23Hz, 3.43Hz and 3.13Hz respectively, with small error, which verifies the correctness of the theoretical calculation method of locked wind speed, and proves that according to different flow rates, The maximum amplitude and output voltage can be obtained by changing the structural parameters of the vibration pickup structure to produce frequency locking phenomenon, which provides a theoretical method and reference for the further engineering design of energy collection structure.

(2) The four kinds of bluff bodies all produce stable vibration with the largest amplitude at the locking wind speed of about 1m/s, and the vibration frequency is about equal to its natural frequency, that is, the locking phenomenon occurs. The 60mm bluff body has the largest vibration amplitude, which is about ±5.6cm, and the energy conversion efficiency reaches 77.38%. In other wind speeds, the amplitude of the system is small and unstable, showing a certain "beat" phenomenon, while the vibration frequency of the blunt body gradually increases with the increase of wind speed. Therefore, further research should focus on broadening the effective wind speed range and effective wind width of the system.

References

[1]XU Zhuo, YANG Jie, YAN Le, CAO Jia-feng, CHEN Xiao-yong,CHOU Xiu-jian. Research progress on micro vibration energy harvesters[J].Transducer and Microsystem Technologies, 2015,34(02):9-12.

[2]ZHANG Zhenyu, SU Yufeng, YE Zhitong.Performance Improvement of Electromagnetic Vibration Energy Harvesters[J].Micronanoelectronic Technology, 2016, 3(11):731-742+772.

[3]ZHANG Duan, WANG Manzhou .Design of HIgh eficiency electromagnetic viebration harvester[J].Journal Of Zhejiang University Of Technology, 018,46(02):168-173.

[4]WEN Yumei, JIANG Xiaofang, LI Ping, YANG Jin, DAI Xianzhi.Vibration Energy Generator Using Composite Magnetoelectric Transduer[J]. Instrument Technique and Sensor,2009(S1):372-375.

[5]LIU Hui, HE Pengju, LINLing, WU Shijie, XIALiang, ZU Yikang.Theoretical Analysis and Simulation of Piezoelectric Continent for Low-Frequeuency Vibration Energy Harvesting

[J].Instrument Technique and Sensor,2009(10):91-93+96.

[6]Wang J , Geng L , Ding L , et al. The state-of-the-art review on energy harvesting of flow-induced vibrations[J]. Applied Energy, 2020.

[7]Yili Hu, Bin Yang, Xiang Chen, Xiaolin Wang, Jingquan Liu,Modeling and experimental study of a piezoelectric energy harvester from vortex shedding-induced vibration,Energy Conversion and Management,Volume 162,2018,145-158.

[8]Jo S , Sun W , Son C , et al. Galloping-based energy harvester considering enclosure effect[J]. AIP Advances, 2018, 8(9):095309.

[9]Sun W , Jo S , Seok J . Development of the optimal bluff body for wind energy harvesting using the synergetic effect of coupled vortex induced vibration and galloping phenomena[J]. International Journal of Mechanical Sciences, 2019.

[10]Junlei Wang, Shengxi Zhou, Zhien Zhang, Daniil Yurchenko,High-performance piezoelectric wind energy harvester with Y-shaped attachments,Energy Conversion and Management,Volume 181,2019, 645-652.

[11Li Baoqing.Experimental Research on Vibration Control of Cylindrical Vortex[D].University of Science and Technology of China,2008.

[12]LI Li,LIN Shanshan, WANG Jinliang, AN Ranran, LU Chenhe, Numerical Simulation of Energy Harvesting Structure of Flexible Circular Tube with Built-in Piezoelectric Cantilever Beam Based on Vortex Induced Vibration[J].Science Technology and Engineering,2020,20(13):5210-5216.

ISSN: 2664-9640

[13]LI Xiaochao, LUO Xuan, XU Wei, FENG Shengnan.Numerical analysis of energy harvesting from flow-induced vibration of cylinders with different cross sections[J].Journal of Harbin Engineering University,2019,40(12):1973-1979.
[14]Ding Daiwei.Two-dimensional numerical simulation of flow around cylinder and vortex-induced vibration[D].Tianjin University,2010..